
GridShow: Omni Visual Generation

Cong Wan^{*1} Xiangyang Luo^{*2} Zijian Cai³ Yiren Song⁴ Yunlong Zhao¹ Yifan Bai^{†1} Yuhang He¹
Yihong Gong¹

Abstract

In this paper, we introduce GRID, a novel paradigm that reframes a broad range of visual generation tasks as the problem of arranging grids, akin to film strips. At its core, GRID transforms temporal sequences into grid layouts, enabling image generation models to process visual sequences holistically. To achieve both layout consistency and motion coherence, we develop a parallel flow-matching training strategy that combines layout matching and temporal losses, guided by a coarse-to-fine schedule that evolves from basic layouts to precise motion control. Our approach demonstrates remarkable efficiency, achieving up to $35\times$ faster inference speeds while using $< \frac{1}{1000}$ of the computational resources compared to specialized models. Extensive experiments show that GRID exhibits exceptional versatility across diverse visual generation tasks, from Text-to-Video to 3D Editing, while maintaining its foundational image generation capabilities. This dual strength in both expanded applications and preserved core competencies establishes GRID as an efficient and versatile **omni-solution** for visual generation. Our code is available at: <https://github.com/Should-AI-Lab/GRID>.

1. Introduction

Film strips demonstrate an elegant approach in visual arts: by arranging temporal sequences into structured grids, allowing time-based narratives to be displayed in layouts while maintaining their narrative coherence and visual connections. This organization does more than preserve chronological order - it enables efficient content manipulation, comparison, and editing. Drawing inspiration from this intuitive yet powerful organizational principle, we propose a fundamental question: **Can we directly reframe various visual generation tasks as how to layout**, where key visual

elements (such as multiple viewpoints or video frames) are treated as grid “layout”?

To answer this, a natural starting point emerges from the recent breakthroughs in text-to-image generation. Models like (Esser et al., 2024; Baldridge et al., 2024; Betker et al., 2023) have shown remarkable capabilities in understanding and generating complex spatial relationships. This leads us to a straightforward initial attempt: we test their ability to generate grid-arranged multi-view layouts through simple prompting (Figure 8). However, our experiments reveal that the current models, despite their advanced capabilities, fall short in two fundamental aspects (detailed in Section A.1):

- **Layout Control:** They fail to maintain both consistent grid structures and visual appearances across layouts.
- **Motion Coherence:** When given specific motion instructions (*e.g.*, “rotate clockwise”), they cannot reliably create sequential movements across layouts.

To address these, we introduce GRID, which **reformulates temporal sequences as grid layouts**, allowing image generation models to process the entire sequence holistically and learn both spatial relationships and motion patterns.

Building on this grid-based framework, we develop a **parallel flow-matching** training strategy that leverages large-scale web datasets, where video frames are arranged in grid layouts. The model learns to simultaneously generate all frames in these structured layouts through a base parallel matching loss, achieving consistent visual appearances and proper grid arrangements. This approach naturally utilizes the models’ self-attention mechanisms to capture and maintain spatial relationships across the entire layout.

For precise motion control, we further incorporate dedicated temporal loss and motion-annotated datasets during fine-tuning. The temporal loss ensures smooth transitions between adjacent frames, while the motion annotations help learn specific patterns like “rotate clockwise”. These components are balanced through a coarse-to-fine training schedule to achieve both fluid motion and consistent spatial structure.

Through our carefully designed training paradigm, GRID achieves remarkable efficiency gains, demonstrating a substantial **6-35 \times** acceleration in inference speed compared

^{*}Equal contribution ¹Xi’an Jiaotong University ²Tsinghua University ³Chinese Academy of Sciences ⁴National University of Singapore. Correspondence to: Yihong Gong <ygong@mail.xjtu.edu.cn>. [†]: Project Lead

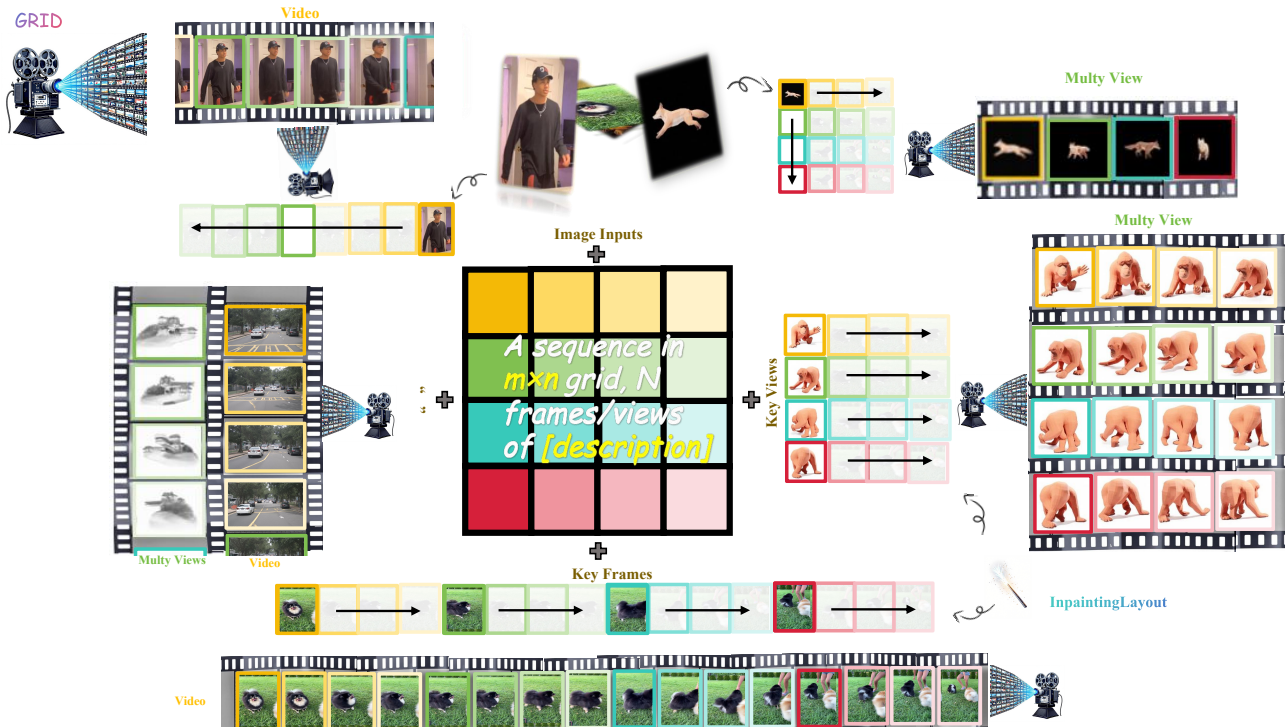


Figure 1: **Framework Overview:** We transform temporal and view sequences into structured layout spaces, enabling consistent synthesis for diverse generation and interpolation tasks from text and image/frame inputs.

to specialized expert models, while requiring merely $\frac{1}{1000}$ of the training computational resources. Our framework exhibits exceptional versatility, achieving competitive or superior performance across a diverse spectrum of generation tasks, including Text-to-Video, Image-to-Video, and Multi-view generations, with performance improvements of up to **23%**. Furthermore, we extend the capabilities of GRID to encompass Video Style Transfer, Video Restoration, and 3D Editing tasks, while preserving its original strong image generation capabilities for image tasks such as image editing and style transfer. This unique combination of expanded capabilities and preserved foundational strengths establishes GRID as a **omni-solution** for visual generation.

Our main contributions are summarized as follows:

- **Novel Grid-based Framework:** We introduce a new paradigm that reformulates temporal sequences as grid layouts, enabling holistic processing of visual sequences through image generation models.
- **Coarse-to-fine Training Strategy:** We develop a parallel flow-matching strategy combining layout matching and temporal coherence losses, with a coarse-to-fine training schedule that evolves from basic layouts to more precise motion control.
- **Omni Generation:** We demonstrate strong performance across multiple visual generation tasks

while maintaining low computational costs. Our method achieves results comparable to task-specific approaches, despite using a single, efficient framework.

2. Layout Generation

Inspired by film strips that organize temporal sequences into structured grids, we present GRID, a grid layout-driven framework that reformulates multiple visual generation tasks through grid-based representation. Our GRID consists of three key components: 1) **Grid Representation**, which enables layout-based video organization for comprehensive visual generation; 2) **Parallel Flow Matching**, which ensures temporal coherence in successive grids; and 3) **Coarse-to-fine Training**, which enhances motion control capabilities. The framework architecture is illustrated in Figure 2 (left).

2.1. Grid Representation

Existing text-to-image models, with inherent attention mechanisms, enable image manipulation and editing by generating new content from partial image information and semantic instructions, which inspires us to extend this capability to temporal generation by introducing a novel input paradigm, termed Grid Representation, that generates temporal content from keyframe visuals and semantic instructions.

Consider a general visual generation task that transforms an input condition $c_{content}$ (such as a text description T) into

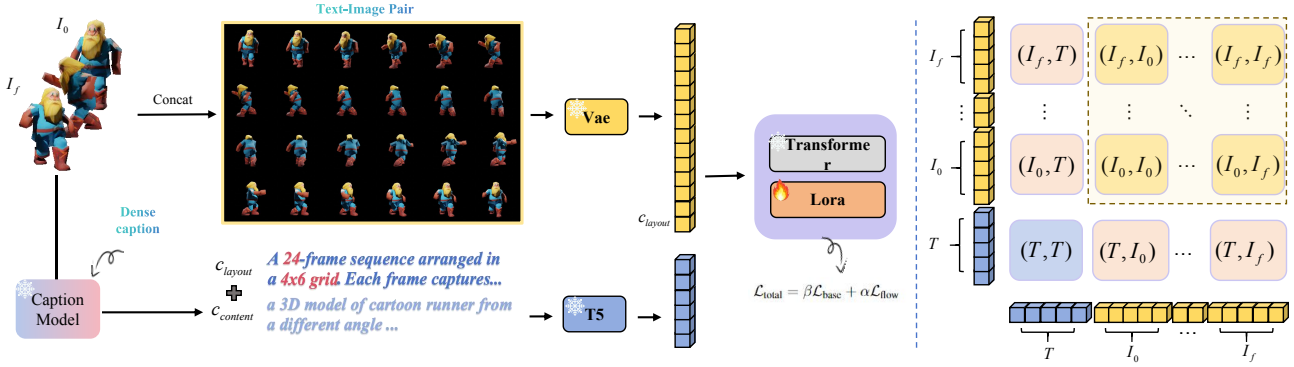


Figure 2: Pipeline Overview. Left: GRID arranges videos into grid layouts, with text annotations describing frame sequences and multi-view spatial relationships. Right: Grid-based reformulation utilizing model’s built-in self-attention.

a sequence of images (I_0, \dots, I_f) . We propose a grid layout specification c_{layout} that arranges temporal frames into a structured grid within a single image, where each cell (i, j) contains a specific image I_{ij} . As shown in Figure 2 (right), when this grid structure is input into a conventional text-to-image model, the model’s inherent attention mechanisms naturally extend their functionality to process this spatial arrangement as:

- **Self-attention Expansion:** The standard self-attention mechanism (I, I) (yellow block) expands into two distinct components:
 - Intra-frame attention (I_i, I_i) : Maintains feature learning within individual grid cells
 - Cross-frame attention (I_i, I_j) : Enables temporal relationships between different grid cells
- **Cross-attention Extension:** The text-image cross-attention (I, T) (pink block) extends naturally to provide uniform text conditioning across all frame positions

Our approach demonstrates that thoughtful problem restructuring can be more effective than architectural modifications. By reorganizing the input space into a grid representation, standard text-to-image models can naturally handle temporal generation without architectural changes (see Appendix A.2 for detailed attention mechanism analysis). This grid-based design offers two key advantages: First, it enables parallel generation of all frames and eliminates the error accumulation problems common in autoregressive approaches (Tian et al., 2024). Second, by leveraging the inherent consistency priors within pretrained image generation models, our approach effectively transfers their learned spatial consistency to temporal and multi-view coherence. This crucial advantage avoids the need for extensive pre-training on massive video datasets, as the grid representation naturally extends existing image-level understanding to

sequence generation. Additionally, through flexible layout conditioning (c_{layout}), our model shows strong generalization capabilities beyond training constraints (Section A.4), suggesting a promising solution to the fixed-length limitations of existing methods. Additionally, our grid representation supports diverse input types, including multi-view images and multi-frame sequences, laying the foundation for a comprehensive omni-generation model that bridges image and video domains.

2.2. Parallel Flow Matching

To fully leverage the potential of our grid representation, we employ parallel flow matching (Esser et al., 2024) to ensure temporal coherence across consecutive grids. For each training sample $\mathbf{I} = (I_{ij})$, we generate a corresponding text representation by integrating layout specifications with content descriptions: $c' = [c_{layout}, c_{content}]$. Here, c_{layout} encodes the spatial structure (e.g., a sequence arranged in $m \times n$ grids), while $c_{content}$ captures the visual content as well as the temporal relationships between frames.

Parallel Flow Evolution with Global Awareness. Our grid representation integrates seamlessly with flow matching by organizing temporal frames into a unified grid image \mathbf{I} . This enables parallel evolution of frames through the following process:

$$\mathbf{I}_t = (1 - t)\mathbf{I} + t\epsilon, \quad t \sim \mathcal{U}(0, 1), \quad \epsilon \sim \mathcal{N}(0, I) \quad (1)$$

Unlike autoregressive approaches that generate frames sequentially, our formulation allows all frames to evolve simultaneously from noise to target distribution through the model’s native prediction process:

$$f : (\mathbf{I}_t, t, c') \rightarrow \epsilon - \mathbf{I} \quad (2)$$

In this formulation, each frame $(I_{ij})_t$ interacts with others within the grid, enabling mutual influence. This interaction naturally enforces temporal consistency across the entire sequence.

2.3. Coarse-to-Fine Training

Training models for temporal understanding in grid representation demands extensive video data to achieve key capabilities like identity preservation and motion consistency - essential features for video and multi-view generation that text-to-image models typically lack. This training process faces two main challenges from mixed quality of available data: the abundance of low-quality internet videos, and high computational costs of processing high-resolution footage. We tackle these limitations through a coarse-to-fine training strategy that combines two key components: data curriculum and loss dynamic. This dual approach optimizes both training efficiency and model performance, enabling effective use of diverse data sources while minimizing computational overhead. Our strategy enhances the capabilities of our flow-based framework without sacrificing training efficiency.

Data Curriculum. Our training strategy follows a Coarse-to-Fine approach, starting with foundational learning and advancing to refinement:

- *Coarse Phase:* In the initial phase, we utilize large-scale Internet datasets, including WebVid, TikTok, and Objaverse, which are designed with uniform c_{layout} specifications. Although the content descriptions (c_{content}) are automatically generated by GLM-4V-9B (Du et al., 2022) and may lack precise control details, the vast scale and diversity of this data—albeit at lower resolutions—provide a strong basis for developing robust spatial understanding and basic layout structures.
- *Fine Phase:* Building on the foundational knowledge from the coarse phase, we transition to training with carefully curated, high-resolution samples. These samples are paired with detailed descriptions generated by GPT-4 (OpenAI, 2023), offering explicit spatial and temporal instructions. As shown in Figure 2, these high-quality captions facilitate fine-grained control over complex layout variations, enabling the model to handle intricate spatial and temporal dynamics effectively.

Loss Dynamic. Alongside the data curriculum, we gradually incorporate temporal supervision by employing a dynamic training objective:

$$\mathcal{L}_{\text{total}} = \mathcal{L}_{\text{base}} + \alpha \mathcal{L}_{\text{flow}} \quad (3)$$

The base loss ensures accurate appearance generation for each grid position:

$$\mathcal{L}_{\text{base}} = \mathbb{E}_{t,\epsilon} [|\epsilon - \epsilon_{\theta}(\mathbf{I}, t, c')|^2] \quad (4)$$

The flow loss captures temporal dynamics through directional changes between adjacent positions:

$$\Delta \epsilon^{ij} = \begin{cases} \epsilon^{ij} - \epsilon^{i,j-1} & \text{if } j > 0 \\ \epsilon^{i,0} - \epsilon^{i-1,n} & \text{if } j = 0 \end{cases} \quad (5)$$

$$\Delta \epsilon_{\theta}^{ij} = \begin{cases} \epsilon_{\theta}^{ij} - \epsilon_{\theta}^{i,j-1} & \text{if } j > 0 \\ \epsilon_{\theta}^{i,0} - \epsilon_{\theta}^{i-1,n} & \text{if } j = 0 \end{cases}$$

$$\mathcal{L}_{\text{flow}} = \mathbb{E}_{t,\epsilon} [|\Delta \epsilon - \Delta \epsilon_{\theta}(\mathbf{I}, t, c')|^2] \quad (6)$$

The weight α gradually increases from 0 to a preset upper bound, allowing the model to first establish precise content generation capabilities before focusing on temporal dynamics. This staged evolution of the loss function complements our data curriculum, enabling the model to effectively learn both the spatial and temporal aspects of generation in a coordinated manner.

2.4. Omni Inference

We propose an omni-inference framework designed to handle a wide range of generation tasks using a reference-guided grid layout initialization. The core idea of our approach is to unify different generation tasks by employing a well-structured initialization process combined with controlled grid noise injection. At the same time, we ensure consistency with the reference through the use of a binary mask.

Given a reference image I_{ref} or key frames (I_0, \dots, I_{m-1}) , we construct a grid structure $\mathbf{I} = (I_{ij})_{m \times n}$. For single-image expansion and frame interpolation tasks, we initialize the grid as:

$$I_{ij} = \begin{cases} I_{\text{ref}} & \text{expansion} \\ (1 - \frac{j}{n})I_{i,0} + \frac{j}{n}I_{i+1,0} & \text{interpolation} \end{cases} \quad (7)$$

The generation process requires both flexibility and reference consistency. To achieve this balance, we introduce controlled grid noise injection instead of starting from pure noise:

$$\mathbf{I}_T = (1 - T)\mathbf{I} + T\epsilon, \quad \epsilon \sim \mathcal{N}(0, I) \quad (8)$$

where T denotes the starting time. This noise injection enables diverse generation while retaining the initialization structure.

To maintain reference consistency during generation, we employ a binary mask $M \in \{0, 1\}^{m \times n}$:

$$M_{ij} = \begin{cases} 0 & \text{if } (i, j) \text{ contains reference frame} \\ 1 & \text{otherwise} \end{cases} \quad (9)$$

This mask modulates the update process:

$$\mathbf{I}_t = (1 - M) \odot \mathbf{I}_{\text{ref}} + M \odot \mathbf{I}_t \quad (10)$$

ensuring reference frames remain unchanged while allowing other regions to evolve.

The noise level T plays a key role in balancing generation quality. A large T leads to pure noise with poor reference consistency, while a small T yields near-duplicates. Our experiments show $T \in [0.8, 1.0]$ a good balance between diversity and fidelity.

3. Experiments

3.1. Experimental Setup

Datasets We train our model separately for video generation and multi-view generation tasks, both following a two-stage strategy: (1) For coarse-level training, we combine video clips from WebVid (Bain et al., 2021), and TikTok (Jafarian & Park, 2022) arranged in 8×8 and 4×4 grid layouts for video generation, and 30K sequences from Objaverse (Deitke et al., 2023) in 4×6 grids for multi-view generation. Each sequence is paired with automated captions and GLM-generated annotations emphasizing spatial and temporal relationships, using the sequence’s inherent attributes (e.g., category labels) and visual content as queries. (2) For fine-grained control, we construct high-quality datasets of 1K sequences with structured annotations for each task. We first manually create exemplar annotations to establish a consistent format, then use these as few-shot examples for GPT-4o to generate precise control instructions while maintaining annotation consistency across the dataset.

Implementation Details We implement GRID based on the FLUX-dev, initializing from its pretrained weights. For video generation training, we adopt LoRA with ranks of 16 and 256, training for 10K steps with batch size 4 across 8 A800 GPUs using AdamW optimizer (learning rate $1e-4$). The temporal loss weight α starts from 0 and gradually increases to a maximum of 0.5. For multi-view generation, we train on 30K sequences for 1.5K steps using LoRA rank 256 and Ours-EF using LoRA rank 16. During inference, we use a guidance scale of 3.5 and sampling step of 20.

Evaluation Protocol We evaluate our model on three distinct generation tasks: (1) Text-to-video generation on UCF-101 dataset (Soomro et al., 2012), evaluated using FVD (Unterthiner et al., 2019) (I3D backbone) and IS (Xu et al., 2018). We evaluate both 16-frame and 64-frame generation settings; (2) Image-to-video generation on a randomly sampled subset of 100 TikTok videos, measured by FVD and CLIP_{img} score; (3) Multi-view generation on Objaverse, where we evaluate on 30 randomly selected objects with 24 frames per sequence at different viewpoints to assess 4D

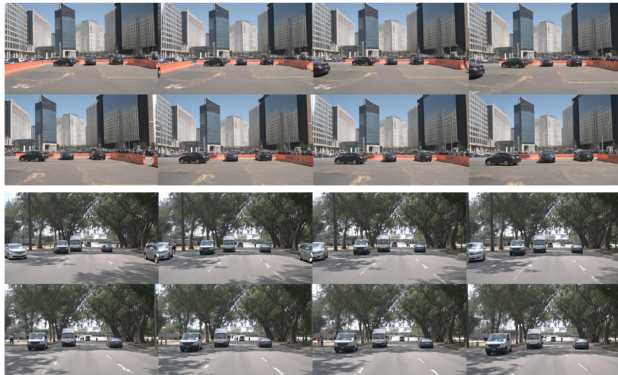


Figure 3: Text-to-Video Generation of driving scenes, showcasing complex multi-vehicle scenarios which represent the most challenging aspects of driving scene generation.



Figure 4: Image-to-Video Generation of dance sequences from TikTok dataset. The leftmost column shows the input reference image, followed by generated motion sequences.

generation capabilities. We compute FVD, CLIP metrics, following (Liang et al., 2024).

3.2. Main Results

We compare our approach with several state-of-the-art methods from well-established video/multiview generation model series, all of which represent the current frontiers in their respective domains.

Text-to-Video Generation As shown in Table 1, we evaluate our approach on both short (16-frame) and long (64-frame) generation tasks. For 16-frame generation, our full model pushes FVD to 418.9, improving the previous best score by 15%, while achieving a 37.34 IS score. More notably, we significantly reduce computational costs, achieving 6.7× faster inference (7.2s vs 48s) compared to CogVideo. This efficiency advantage becomes more

Table 1: **Comprehensive Generation Results.** Comparison across different generation tasks. Our model demonstrates superior efficiency while maintaining competitive quality across varying sequence lengths. Notably, while existing methods (AnimateDiffv3, VideoCrafter2) are limited to 16-frame generation, our approach scales efficiently to 64-frame sequences with only linear time increase. Underlined values indicate the best results among our variants, and bold values show the best across all methods. Test Time indicates the average sampling time per sequence.

Method	Text-to-Video (16-frame)			Text-to-Video (64-frame)			Image-to-Video	
	FVD↓	IS↑	Test Time(s)↓	FVD↓	IS↑	Test Time(s)↓	FVD↓	CLIP _{img} ↑
AnimateDiffv3	464.1	35.24	12	-	-	-	250.9	0.9229
VideoCrafter2	424.2	32.00	15	-	-	-	-	-
OpenSora1.2	472.0	39.07	12	1000.5	37.11	66	-	-
CogVideo5b	301.1	36.27	48	740.1	34.82	132	122.5	0.9185
Ours(Stage1)	482.1	32.46	7.2	1003.2	32.48	24	115.5	0.9598
Ours(Stage1+2)	438.3	36.56	7.2	994.6	36.47	24	104.6	0.9695
Ours(Full)	<u>418.9</u>	<u>37.34</u>	<u>7.2</u>	<u>787.1</u>	<u>36.63</u>	<u>24</u>	93.7	0.9709

Table 2: Quantitative comparison of Multi-view Generation Results on Text-to-Multiview, Image-to-Multiview and Multiview interpolation Tasks. Time indicates the whole time cost during inference

Task	Method	CLIP-F↑	CLIP-O↑	FVD↓	Time↓
Text 2MV	4DFY	0.8092	0.6163	390.4	3h
	Ours-EF	0.9060	0.6189	355.6	6m
	Ours	0.9427	0.6247	324.3	6m
Image 2MV	STAG4D	0.88	0.64	475.4	3h30m
	Ours-EF	0.9392	0.6580	333.7	6m
	Ours	0.9486	0.6554	350.6	6m
Interp olation	Ours-EF	0.9356	0.7223	348.2	6m
	Ours	0.9543	0.7415	295.1	6m

pronounced in 64-frame generation, where our approach maintains 5.5× faster inference speed. Our staged training demonstrates clear benefits: Stage1 (trained with coarse annotations and \mathcal{L}_{base} only) achieves a FVD of 482.1, which reduces to 438.3 with fine-grained annotations, and further reduces to 418.9 with \mathcal{L}_{flow} .

Image-to-Video Generation We evaluate on the TikTok dataset, which contains 100 high-quality short videos with diverse motion patterns after our processing and annotation process. For image-guided video synthesis, our method achieves breakthrough performance by reducing FVD to 93.7, a 23% improvement over the second-best result. The CLIP_{img} score also sees a substantial boost to 0.9709.

Multi-view Generation We evaluate multi-view generation capabilities on selected Objaverse test set, which contains 30 3D objects from multiple viewpoints. As shown in Table 2, our method achieves transformative improvements in text-to-multi-view synthesis. We improve CLIP-F

score by 13.4 points to 0.9427 and reduce FVD by 17% to 324.3, while dramatically cutting inference time from 3 hours to just 6 minutes compared to 4DFY (Bahmani et al., 2024). For image-to-multi-view tasks, we push the CLIP-F score up by 6.9 points to 0.9486 while achieving 35× faster inference compared to STAG4D (Zeng et al., 2024).

3.3. Extension Capabilities

Beyond the primary generation tasks, we demonstrate GRID’s strong zero-shot generalization capabilities across diverse video and multi-view applications without any task-specific training or architectural modifications. The layout-based design enables natural adaptation to various downstream tasks through prompt engineering alone.

Video Style Transfer We explore zero-shot style transfer capabilities. As shown in Figure 6, our model successfully transfers distinctive features from fox, red panda, and tiger while maintaining the original temporal coherence and motion patterns.

Video Restoration Our architecture’s multi-scale processing capability enables effective video restoration without explicit training. Figure 12 shows our model’s performance in recovering high-quality videos from severely degraded inputs (with Gaussian blur and block masking).

3D Editing We further showcase the model’s understanding of 3D structure through zero-shot appearance editing. As demonstrated in Figure 7, given a sequence of human poses, our model can generate diverse variations by controlling attributes like hair color and clothing style through simple text. This capability stems from our layout-based training strategy, which naturally captures the relationship between spatial arrangement and semantic attributes.

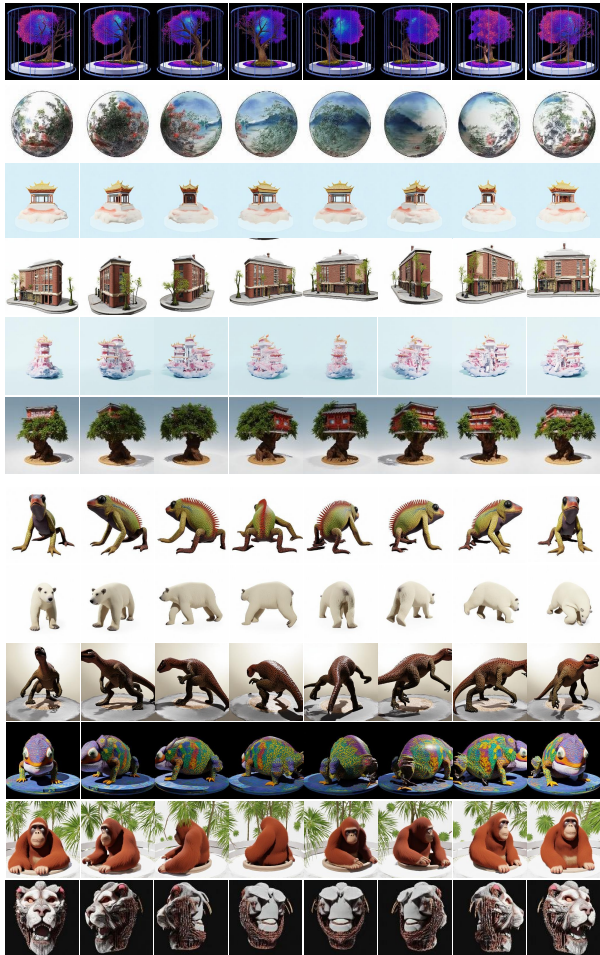


Figure 5: Multi-view generation results for static objects (top six rows) and dynamic subjects (bottom six rows), demonstrating consistent appearance and structure across different viewpoints.

These extensions validate the strong generalization potential of our approach. By leveraging the grid-based architecture and rich layout representations learned during training, GRID adapts to various downstream tasks without modifications, offering a versatile foundation for video and multi-view applications. More potential applications are demonstrated in Appendix A.6. Furthermore, since our method preserves FLUX’s original architecture, it retains all image generation capabilities of the base model, as shown in Appendix A.6.4.

4. Related Work

Text-to-Image Generation Diffusion models (Sohl-Dickstein et al., 2015; Ho et al., 2020) have fundamentally transformed image generation by employing iterative denoising processes to synthesize high-quality outputs. Subsequent advancements (Rombach et al., 2022; Podell et al.,

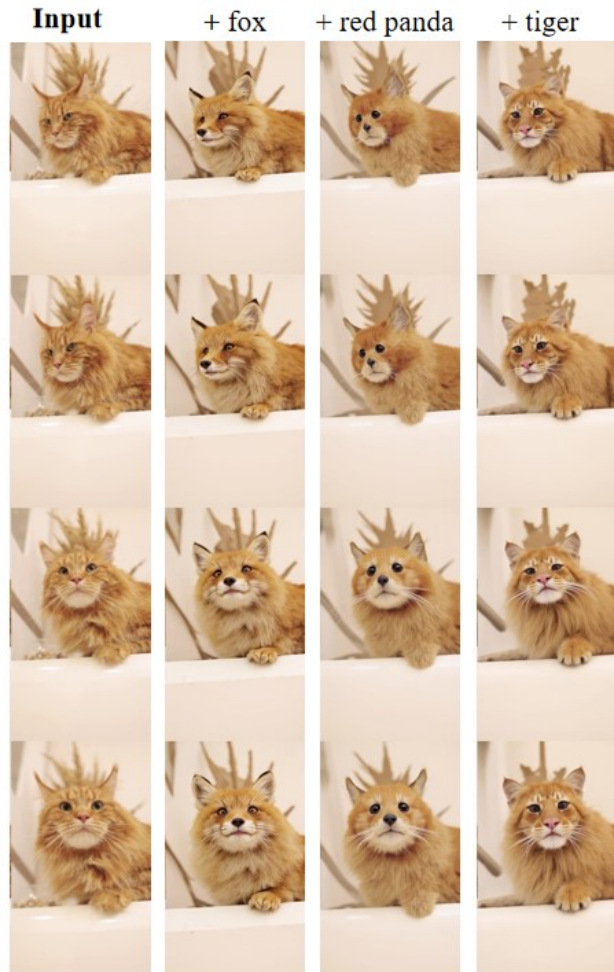


Figure 6: Zero-shot video style transfer results. Our model incorporates characteristics from different animals (fox, red panda, tiger) while maintaining motion coherence.

2023; Ramesh et al., 2022; Saharia et al., 2022) have refined this paradigm leveraging latent spaces with significantly reduced computational costs. Diffusion Transformers (DiT) (Peebles & Xie, 2023) further advanced this area by replacing the U-Net architecture with transformer-based designs. This architectural shift improved training efficiency, paving the way for more scalable and versatile generative frameworks. Building on these, flow matching (Lipman et al., 2022; Esser et al., 2024) reformulates the generation process as a straight-path trajectory between data and noise distributions. More recently, FLUX (BlackForest, 2024), has combined the strengths of DiT and flow matching to achieve efficient and high-quality image generation. These models also integrate powerful language models (Raffel et al., 2020) and joint text-image attention mechanisms. This multimodal understanding has unlocked new possibilities for instruction-following and creative applications. Beyond generating high-quality images, text-to-image mod-



Figure 7: Zero-shot 3D editing with attribute control. Our model generates diverse variations by modifying appearance attributes through text prompts while preserving motion patterns.

els demonstrate a strong spatial understanding that can be naturally extended to temporal dimensions through layout representations, enabling diverse downstream tasks.

Task-Specific Generation Diffusion-based approaches have shown remarkable progress in generalized video generation tasks (Ho et al., 2022; Blattmann et al., 2023b; Zhang et al., 2023; Blattmann et al., 2023a; He et al., 2023; Zhou et al., 2022; Wang et al., 2023a; Ge et al., 2023; Wang et al., 2023c;b; Singer et al., 2022; Zhang et al., 2023; Zeng et al., 2023). Notable works like VideoLDM (Blattmann et al., 2023b), Animatediff (Guo et al., 2023), and SVD (Chai et al., 2023) advance temporal modeling through specialized architectures. In the multi-view domain, various approaches (Watson et al., 2022; Liu et al., 2023a; Shi et al., 2023b; Long et al., 2024; Shi et al., 2023a; Lu et al., 2024; Li et al., 2023; Liu et al., 2023b; Li et al., 2024; Yang et al., 2024) focus on cross-view consistency through different attention mechanisms and feature space alignments. Recent 4D generation methods (Ren et al., 2023; Liang et al., 2024; Xie et al., 2024b; Sun et al., 2024; Wu et al., 2024) further extend to joint spatial-temporal synthesis, though often facing efficiency challenges or requiring multi-step generation. While these methods achieve remarkable results, they are

typically tailored to specific tasks, relying on specialized architectures for image, video, or multi-view generation. Additionally, methods like VideoPoet (Kondratyuk et al., 2023) employ complex cross-modal alignment mechanisms to bridge different generation modes. In contrast, our approach introduces layout generation, an omni framework that transforms temporal and spatial generation into layout representations. This enables seamless multi-modal generation, to address a wide range of tasks through straightforward modifications to input representations, without the need for complex cross-modal alignment mechanisms.

5. Conclusion

We present GRID, a unified layout-based framework bridging video and multi-view generation through efficient grid representation. Our two-stage training strategy enables both robust generation and precise control, while the temporal refinement mechanism enhances motion coherence. Experiments demonstrate significant computational efficiency gains while maintaining competitive performance across tasks. The framework’s strong zero-shot generalization capabilities further enable adaptation to diverse applications without task-specific training, suggesting a promising direction for efficient visual sequence generation.

Impact Statement

This paper introduces research aimed at advancing visual sequence generation through an efficient layout-based framework. However, we must emphasize the potential risks associated with this technology, particularly in facial manipulation applications (Xie et al., 2024a; Luo et al., 2024), where our method could be misused to compromise identity security. Nevertheless, recent advances in adversarial perturbation protection mechanisms (Wan et al., 2024) provide solutions to help users protect their personal data against unauthorized model fine-tuning and malicious content generation. Therefore, we call for attention to these risks and encourage the adoption of defensive techniques to ensure the protection of personal content while advancing the development of generative AI technologies.

References

- Bahmani, S., Skorokhodov, I., Rong, V., Wetzstein, G., Guibas, L., Wonka, P., Tulyakov, S., Park, J. J., Tagliasacchi, A., and Lindell, D. B. 4d-fy: Text-to-4d generation using hybrid score distillation sampling. *IEEE Conference on Computer Vision and Pattern Recognition (CVPR)*, 2024.
- Bai, Y., Wu, D., Liu, Y., Jia, F., Mao, W., Zhang, Z., Zhao, Y., Shen, J., Wei, X., Wang, T., et al. Is a 3d-tokenized llm the key to reliable autonomous driving? *arXiv preprint arXiv:2405.18361*, 2024.
- Bain, M., Nagrani, A., Varol, G., and Zisserman, A. Frozen in time: A joint video and image encoder for end-to-end retrieval. In *Proceedings of the IEEE/CVF international conference on computer vision*, pp. 1728–1738, 2021.
- Baldridge, J., Bauer, J., Bhutani, M., Brichtova, N., Bunner, A., Chan, K., Chen, Y., Dieleman, S., Du, Y., Eaton-Rosen, Z., et al. Imagen 3. *arXiv preprint arXiv:2408.07009*, 2024.
- Betker, J., Goh, G., Jing, L., Brooks, T., Wang, J., Li, L., Ouyang, L., Zhuang, J., Lee, J., Guo, Y., et al. Improving image generation with better captions. *Computer Science*. <https://cdn.openai.com/papers/dall-e-3.pdf>, 2(3):8, 2023.
- BlackForest. Flux. <https://github.com/black-forest-labs/flux>, 2024.
- Blattmann, A., Dockhorn, T., Kulal, S., Mendeleevitch, D., Kilian, M., Lorenz, D., Levi, Y., English, Z., Voleti, V., Letts, A., et al. Stable video diffusion: Scaling latent video diffusion models to large datasets. *arXiv preprint arXiv:2311.15127*, 2023a.
- Blattmann, A., Rombach, R., Ling, H., Dockhorn, T., Kim, S. W., Fidler, S., and Kreis, K. Align your latents: High-resolution video synthesis with latent diffusion models. In *CVPR*, pp. 22563–22575, 2023b.
- Chai, W., Guo, X., Wang, G., and Lu, Y. Stablevideo: Text-driven consistency-aware diffusion video editing. In *CVPR*, pp. 23040–23050, 2023.
- Deitke, M., Schwenk, D., Salvador, J., Weihs, L., Michel, O., VanderBilt, E., Schmidt, L., Ehsani, K., Kembhavi, A., and Farhadi, A. Objaverse: A universe of annotated 3d objects. In *Proceedings of the IEEE/CVF Conference on Computer Vision and Pattern Recognition*, pp. 13142–13153, 2023.
- Du, Z., Qian, Y., Liu, X., Ding, M., Qiu, J., Yang, Z., and Tang, J. GLM: general language model pretraining with autoregressive blank infilling. pp. 320–335, 2022.
- Esser, P., Kulal, S., Blattmann, A., Entezari, R., Müller, J., Saini, H., Levi, Y., Lorenz, D., Sauer, A., Boesel, F., et al. Scaling rectified flow transformers for high-resolution image synthesis. In *Forty-first International Conference on Machine Learning*, 2024.
- Ge, S., Nah, S., Liu, G., Poon, T., Tao, A., Catanzaro, B., Jacobs, D., Huang, J.-B., Liu, M.-Y., and Balaji, Y. Preserve your own correlation: A noise prior for video diffusion models. In *CVPR*, pp. 22930–22941, 2023.
- Guo, Y., Yang, C., Rao, A., Wang, Y., Qiao, Y., Lin, D., and Dai, B. Animatediff: Animate your personalized text-to-image diffusion models without specific tuning. *arXiv preprint arXiv:2307.04725*, 2023.
- He, Y., Yang, T., Zhang, Y., Shan, Y., and Chen, Q. Latent video diffusion models for high-fidelity long video generation. *arXiv preprint arXiv:2211.13221*, 2(3):4, 2023.
- Ho, J., Jain, A., and Abbeel, P. Denoising diffusion probabilistic models. *Advances in neural information processing systems*, 33:6840–6851, 2020.
- Ho, J., Chan, W., Saharia, C., Whang, J., Gao, R., Gritsenko, A., Kingma, D. P., Poole, B., Norouzi, M., Fleet, D. J., et al. Imagen video: High definition video generation with diffusion models. *arXiv preprint arXiv:2210.02303*, 2022.
- Jafarian, Y. and Park, H. S. Self-supervised 3d representation learning of dressed humans from social media videos. *IEEE Transactions on Pattern Analysis and Machine Intelligence*, 45(7):8969–8983, 2022.
- Kondratyuk, D., Yu, L., Gu, X., Lezama, J., Huang, J., Schindler, G., Hornung, R., Birodkar, V., Yan, J., Chiu, M.-C., et al. Videopoet: A large language model for zero-shot video generation. *arXiv preprint arXiv:2312.14125*, 2023.
- Li, J., Tan, H., Zhang, K., Xu, Z., Luan, F., Xu, Y., Hong, Y., Sunkavalli, K., Shakhnarovich, G., and Bi, S. Instant3d: Fast text-to-3d with sparse-view generation and large reconstruction model. *arXiv preprint arXiv:2311.06214*, 2023.
- Li, P., Liu, Y., Long, X., Zhang, F., Lin, C., Li, M., Qi, X., Zhang, S., Luo, W., Tan, P., et al. Era3d: High-resolution multiview diffusion using efficient row-wise attention. *arXiv preprint arXiv:2405.11616*, 2024.
- Liang, H., Yin, Y., Xu, D., Liang, H., Wang, Z., Plataniotis, K. N., Zhao, Y., and Wei, Y. Diffusion4d: Fast spatial-temporal consistent 4d generation via video diffusion models. *arXiv preprint arXiv:2405.16645*, 2024.
- Lipman, Y., Chen, R. T., Ben-Hamu, H., Nickel, M., and Le, M. Flow matching for generative modeling. *arXiv preprint arXiv:2210.02747*, 2022.
- Liu, R., Wu, R., Van Hoorick, B., Tokmakov, P., Zakharov, S., and Vondrick, C. Zero-1-to-3: Zero-shot one image to 3d object. In *Proceedings of the IEEE/CVF international conference on computer vision*, pp. 9298–9309, 2023a.

- Liu, Y., Lin, C., Zeng, Z., Long, X., Liu, L., Komura, T., and Wang, W. Syncdreamer: Generating multiview-consistent images from a single-view image. *arXiv preprint arXiv:2309.03453*, 2023b.
- Long, X., Guo, Y.-C., Lin, C., Liu, Y., Dou, Z., Liu, L., Ma, Y., Zhang, S.-H., Habermann, M., Theobalt, C., et al. Wonder3d: Single image to 3d using cross-domain diffusion. In *Proceedings of the IEEE/CVF Conference on Computer Vision and Pattern Recognition*, pp. 9970–9980, 2024.
- Lu, Y., Zhang, J., Li, S., Fang, T., McKinnon, D., Tsin, Y., Quan, L., Cao, X., and Yao, Y. Direct2. 5: Diverse text-to-3d generation via multi-view 2.5 d diffusion. In *Proceedings of the IEEE/CVF Conference on Computer Vision and Pattern Recognition*, pp. 8744–8753, 2024.
- Luo, X., Zhang, X., Xie, Y., Tong, X., Yu, W., Chang, H., Ma, F., and Yu, F. R. Codeswap: Symmetrically face swapping based on prior codebook. In *Proceedings of the 32nd ACM International Conference on Multimedia*, pp. 6910–6919, 2024.
- OpenAI. GPT-4 technical report. *arXiv:2303.08774*, 2023.
- Peebles, W. and Xie, S. Scalable diffusion models with transformers. In *Proceedings of the IEEE/CVF International Conference on Computer Vision*, pp. 4195–4205, 2023.
- Podell, D., English, Z., Lacey, K., Blattmann, A., Dockhorn, T., Müller, J., Penna, J., and Rombach, R. Sdxl: Improving latent diffusion models for high-resolution image synthesis. *arXiv preprint arXiv:2307.01952*, 2023.
- Raffel, C., Shazeer, N., Roberts, A., Lee, K., Narang, S., Matena, M., Zhou, Y., Li, W., and Liu, P. J. Exploring the limits of transfer learning with a unified text-to-text transformer. *Journal of Machine Learning Research*, 21(1):5485–5551, 2020.
- Ramesh, A., Dhariwal, P., Nichol, A., Chu, C., and Chen, M. Hierarchical text-conditional image generation with clip latents. *arXiv preprint arXiv:2204.06125*, 1(2):3, 2022.
- Ren, J., Pan, L., Tang, J., Zhang, C., Cao, A., Zeng, G., and Liu, Z. Dreamgaussian4d: Generative 4d gaussian splatting. *arXiv preprint arXiv:2312.17142*, 2023.
- Rombach, R., Blattmann, A., Lorenz, D., Esser, P., and Ommer, B. High-resolution image synthesis with latent diffusion models. In *Proceedings of the IEEE/CVF conference on computer vision and pattern recognition*, pp. 10684–10695, 2022.
- Saharia, C., Chan, W., Saxena, S., Li, L., Whang, J., Denton, E., Ghasemipour, S. K. S., Karagol Ayan, B., Mahdavi, S. S., Gontijo Lopes, R., Salimans, T., Ho, J., Fleet, D., and Norouzi, M. Imagen: unprecedented photorealism \times deep level of language understanding, 2022.
- Shi, R., Chen, H., Zhang, Z., Liu, M., Xu, C., Wei, X., Chen, L., Zeng, C., and Su, H. Zero123++: a single image to consistent multi-view diffusion base model. *arXiv preprint arXiv:2310.15110*, 2023a.
- Shi, Y., Wang, P., Ye, J., Long, M., Li, K., and Yang, X. Mvdream: Multi-view diffusion for 3d generation. *arXiv preprint arXiv:2308.16512*, 2023b.
- Singer, U., Polyak, A., Hayes, T., Yin, X., An, J., Zhang, S., Hu, Q., Yang, H., Ashual, O., Gafni, O., et al. Make-a-video: Text-to-video generation without text-video data. *arXiv preprint arXiv:2209.14792*, 2022.
- Sohl-Dickstein, J., Weiss, E., Maheswaranathan, N., and Ganguli, S. Deep unsupervised learning using nonequilibrium thermodynamics. In *International conference on machine learning*, pp. 2256–2265. PMLR, 2015.
- Soomro, K., Zamir, A. R., and Shah, M. Ucf101: A dataset of 101 human actions classes from videos in the wild. *arXiv preprint arXiv:1212.0402*, 2012.
- Sun, W., Chen, S., Liu, F., Chen, Z., Duan, Y., Zhang, J., and Wang, Y. Dimensionx: Create any 3d and 4d scenes from a single image with controllable video diffusion. *arXiv preprint arXiv:2411.04928*, 2024.
- Tian, K., Jiang, Y., Yuan, Z., Peng, B., and Wang, L. Visual autoregressive modeling: Scalable image generation via next-scale prediction. *arXiv preprint arXiv:2404.02905*, 2024.
- Unterthiner, T., van Steenkiste, S., Kurach, K., Marinier, R., Michalski, M., and Gelly, S. Fvd: A new metric for video generation. 2019.
- Wan, C., He, Y., Song, X., and Gong, Y. Prompt-agnostic adversarial perturbation for customized diffusion models. *arXiv preprint arXiv:2408.10571*, 2024.
- Wang, J., Yuan, H., Chen, D., Zhang, Y., Wang, X., and Zhang, S. Modelscope text-to-video technical report. *arXiv preprint arXiv:2308.06571*, 2023a.
- Wang, W., Yang, H., Tuo, Z., He, H., Zhu, J., Fu, J., and Liu, J. Videofactory: Swap attention in spatiotemporal diffusions for text-to-video generation. *arXiv preprint arXiv:2305.10874*, 2023b.
- Wang, X., Xie, L., Dong, C., and Shan, Y. Real-esrgan: Training real-world blind super-resolution with pure synthetic data. In *International Conference on Computer Vision Workshops (ICCVW)*.
- Wang, Y., He, Y., Li, Y., Li, K., Yu, J., Ma, X., Chen, X., Wang, Y., Luo, P., Liu, Z., et al. Internvid: A large-scale video-text dataset for multimodal understanding and generation. *arXiv preprint arXiv:2307.06942*, 2023c.
- Watson, D., Chan, W., Martin-Brualla, R., Ho, J., Tagliasacchi, A., and Norouzi, M. Novel view synthesis with diffusion models. *arXiv preprint arXiv:2210.04628*, 2022.
- Wu, R., Gao, R., Poole, B., Trevithick, A., Zheng, C., Barron, J. T., and Holynski, A. Cat4d: Create anything in 4d with multi-view video diffusion models. *arXiv preprint arXiv:2411.18613*, 2024.
- Xie, Y., Xu, H., Song, G., Wang, C., Shi, Y., and Luo, L. X-portrait: Expressive portrait animation with hierarchical motion attention. In *ACM SIGGRAPH 2024 Conference Papers*, pp. 1–11, 2024a.
- Xie, Y., Yao, C.-H., Voleti, V., Jiang, H., and Jampani, V. Sv4d: Dynamic 3d content generation with multi-frame and multi-view consistency. *arXiv preprint arXiv:2407.17470*, 2024b.
- Xu, Q., Huang, G., Yuan, Y., Guo, C., Sun, Y., Wu, F., and Weinberger, K. An empirical study on evaluation metrics of generative adversarial networks. *arXiv preprint arXiv:1806.07755*, 2018.

Yang, X., Shi, H., Zhang, B., Yang, F., Wang, J., Zhao, H., Liu, X., Wang, X., Lin, Q., Yu, J., et al. Hunyuan3d-1.0: A unified framework for text-to-3d and image-to-3d generation. *arXiv preprint arXiv:2411.02293*, 2024.

Zeng, Y., Wei, G., Zheng, J., Zou, J., Wei, Y., Zhang, Y., and Li, H. Make pixels dance: High-dynamic video generation. *arXiv preprint arXiv:2311.10982*, 2023.

Zeng, Y., Jiang, Y., Zhu, S., Lu, Y., Lin, Y., Zhu, H., Hu, W., Cao, X., and Yao, Y. Stag4d: Spatial-temporal anchored generative 4d gaussians. 2024.

Zhang, D. J., Wu, J. Z., Liu, J.-W., Zhao, R., Ran, L., Gu, Y., Gao, D., and Shou, M. Z. Show-1: Marrying pixel and latent diffusion models for text-to-video generation. *arXiv preprint arXiv:2309.15818*, 2023.

Zhou, D., Wang, W., Yan, H., Lv, W., Zhu, Y., and Feng, J. Magicvideo: Efficient video generation with latent diffusion models. *arXiv preprint arXiv:2211.11018*, 2022.

A. Appendix

A.1. Why Flux? Zero-shot Analysis of Foundation Models

To better understand the layout capabilities of existing models before fine-tuning, we conducted a comprehensive zero-shot evaluation comparing three state-of-the-art models: DALLE-3, Flux, and Imagen3. Figure 8 presents their generation results, with each row corresponding to DALLE-3 (top), Flux (middle), and Imagen3 (bottom) respectively.

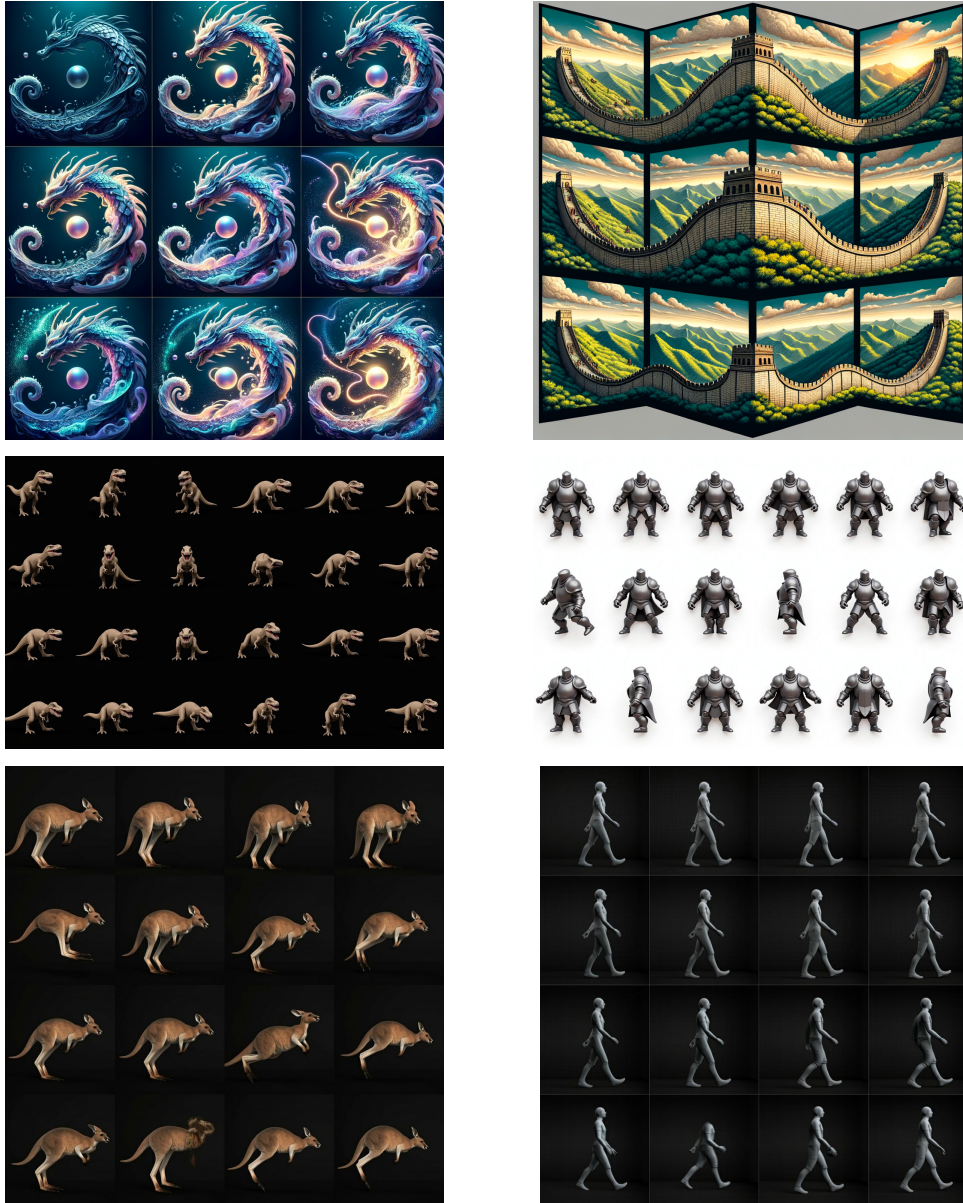


Figure 8: Zero-shot evaluation of foundation models on grid-based multi-view generation tasks before we begin to train. Using the prompt "a * from different angles in a mxn grid layout," First row: Dalle3, Second row: Flux, Third row: Imagen3.

Our analysis reveals varying degrees of grid layout understanding across models. While all models demonstrate basic grid comprehension, they exhibit different strengths and limitations. For motion control, we observe that precise directional instructions (e.g., clockwise rotation) often result in random orientations across all models, indicating limited spatial-temporal control capabilities.

In terms of grid structure accuracy, DALLE-3 shows inconsistent interpretation of specific layout requirements (e.g., 4x4 or

4x6 grids), while Flux and Imagen3 demonstrate better adherence to specified grid configurations. Notably, Flux exhibits superior understanding of spatial arrangements.

Content consistency across grid cells varies significantly. Both Imagen3 and DALLE-3 show noticeable variations in object appearance across frames, while Flux maintains better consistency in object characteristics throughout the sequence. This superior consistency, combined with its open-source nature, motivated our choice of Flux as the base model for our framework.

A.2. Why is it Natural for GRID to Leverage Built-in Attention Mechanism

Video generation fundamentally requires three key capabilities: spatial understanding within frames, temporal consistency between frames, and semantic control across the entire sequence. Traditional approaches tackle these requirements by implementing separate attention modules, as shown in Figure 9(a). While this modular design directly addresses each requirement, it introduces architectural complexity and potential inconsistencies between modules.

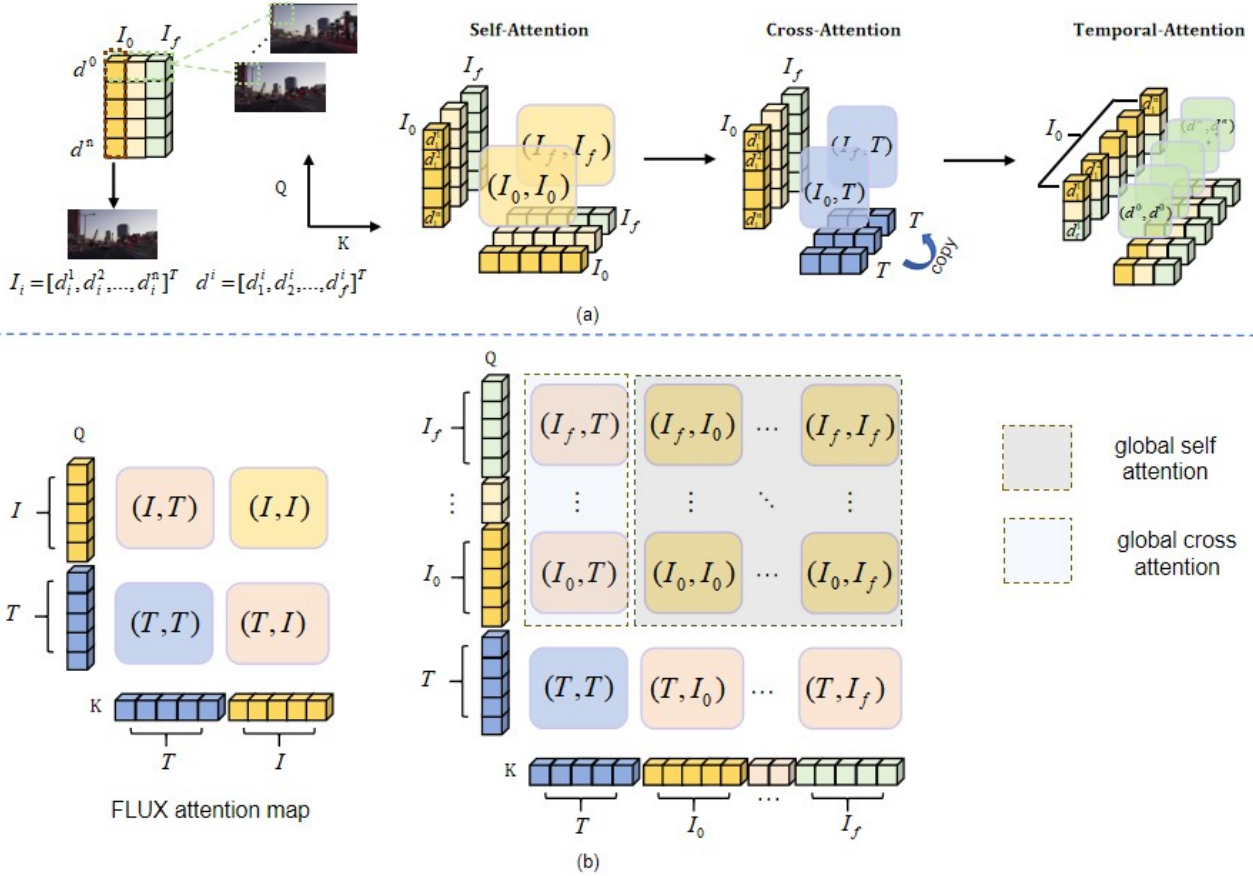


Figure 9: Comparison of attention mechanisms. (a) Traditional video diffusion models rely on three separate attention modules to handle spatial understanding, semantic guidance, and temporal consistency respectively. (b) Through our grid layout reformulation, FLUX’s unified self-attention naturally encompasses both inner-frame (I_i, I_j) and cross-frame (I_i, I_j) relationships, while its global text-image attention (T, I) enables consistent control across all frames. This simplification eliminates the need for specialized temporal modules while maintaining effective spatio-temporal understanding.

Our key insight is that these seemingly distinct requirements can be unified through spatial reformulation. By organizing temporal sequences into grid layouts, we transform temporal relationships into spatial ones, allowing FLUX’s native attention mechanism to naturally handle all requirements through a single, coherent process.

This unification works through two complementary mechanisms, as illustrated in Figure 9(b). First, the original image self-attention (I, I) automatically extends across the grid structure. When processing grid cells containing different temporal

frames, this self-attention naturally splits into inner-frame attention (I_i, I_i) and cross-frame attention (I_i, I_j) . The inner-frame component maintains spatial understanding within each frame, while the cross-frame component captures temporal relationships - effectively handling both spatial and temporal coherence through a single mechanism.

Second, the text-image cross-attention $(T, [I_i]_{i=0}^f)$ operates globally across all grid cells, enabling unified semantic control. This global operation ensures that textual instructions consistently influence all frames, maintaining semantic coherence throughout the sequence. The grid layout allows this semantic guidance to naturally incorporate both content and temporal specifications, as the attention mechanism can reference the spatial relationships between grid cells.

This reformulation fundamentally changes how temporal information is processed. Rather than treating temporal relationships as a separate problem requiring specialized mechanisms, we transform them into spatial relationships that existing attention mechanisms are already optimized to handle. This approach not only simplifies the architecture but also provides more robust temporal understanding, as it leverages the well-established capabilities of spatial attention mechanisms.

The elegance of this solution lies in its ability to achieve complex temporal processing without architectural modifications. By thoughtfully restructuring the problem space, we enable standard attention mechanisms to naturally extend their capabilities, demonstrating how strategic problem reformulation can be more powerful than architectural elaboration.

A.3. Computational Efficiency Analysis

Current state-of-the-art video generation models require extensive computational resources. CogVideo utilizes approximately 35M video clips with an additional 2B filtered images from LAION-5B and COYO-700M datasets. Open-Sora operates on more than 30M videos and demands multiple 80GB GPUs with sequence parallelism for inference.

In contrast, GRID achieves competitive performance with less than 35K training videos and requires only 160M-2560M additional parameters. This significant reduction in resource requirements stems from our grid-based architecture and targeted training strategy. Specifically, our architecture enables efficient parallel processing and parameter sharing, while our training approach focuses on essential video-specific components while leveraging pretrained image capabilities.

The efficiency improvements can be quantified through the following key aspects:

$$\text{Data Reduction} \approx \frac{> 35M}{< 35K} = 1000\times \tag{11}$$

These improvements enable high-quality video generation while maintaining accessibility for research environments with limited computational resources.

A.4. Inference Details

For extension tasks (style transfer, restoration, and editing), we modify the omni-inference framework to process full sequences while maintaining temporal coherence. Unlike the reference-guided generation that requires partial initialization and masking, these tasks operate on complete sequences with controlled noise injection for appearance modification.

Given an input sequence represented as a grid structure $\mathbf{I} = (I_{ij})_{m \times n}$, we initialize the generation process with noise-injected states:

$$\mathbf{I}_T = (1 - T)\mathbf{I} + T\epsilon, \quad \epsilon \sim \mathcal{N}(0, I) \tag{12}$$

where $T \in [0.8, 0.9]$ represents a lower noise level compared to the reference-guided generation. This lower T value helps preserve the original temporal structure while allowing sufficient flexibility for appearance modifications.

A.5. Post-Processing Pipeline

For multi-view generation results, we employ a two-stage enhancement process. First, the generated sequences are processed as video frames to ensure temporal consistency. Subsequently, we apply super-resolution using Real-ESRGAN (Wang et al.) with anime-video-v3 weights, upscaling from 256x256 resolution to 1024x1024. This enhancement pipeline significantly improves visual quality while maintaining temporal coherence.

Table 3 shows parts of our inference prompts for multiview generation. We basically follow this prompt format.

Common Format	A 24-frame sequence arranged in a 4x6 grid. Each frame captures a 3D model of [subject] from a different angle, rotating 360 degrees. The sequence begins with a front view and progresses through a complete clockwise rotation
Category	Subject Description
Creative Fusion	<p>a skyscraper with knitted wool surface and cable-knit details</p> <p>a mechanical hummingbird with clockwork wings and steampunk gears hovering near a neon flower</p> <p>a bonsai tree with spiral galaxies and nebulae blooming from its twisted branches</p> <p>a phoenix crafted entirely from woven bamboo strips with intricate basketwork details glowing from within</p> <p>a jellyfish with a transparent porcelain bell decorated in blue-and-white patterns and ink-brush tentacles</p> <p>a coral reef made entirely of rainbow-hued blown glass with intricate marine life formations</p> <p>an urban street where buildings are shaped as giant functional musical instruments including a violin apartment and piano mall</p> <p>a butterfly with stained glass wings depicting medieval scenes catching sunlight</p> <p>a floating city where traditional Chinese pavilions rest on clouds made of flowing silk fabric in pastel colors</p> <p>a lion composed of moving gears and pistons that transforms between mechanical and organic forms</p> <p>a garden where geometric crystal formations grow and branch like plants with rainbow refractions</p> <p>a tree whose trunk is a twisting pagoda with branches of miniature traditional buildings and roof tile leaves</p> <p>a phoenix-dragon hybrid creature covered in mirrored scales that create fractal reflections</p> <p>a celestial teapot with constellation etchings pouring a stream of stars and nebulae</p> <p>an origami landscape where paper mountains continuously fold and unfold to reveal geometric cities and rivers</p> <p>a sphere where traditional Chinese ink and wash paintings flow continuously between day and night scenes</p>
Natural Creatures	<p>a Velociraptor in hunting pose with detailed scales and feathers</p> <p>a Mammoth with detailed fur and tusks</p> <p>a chameleon changing colors with detailed scales</p> <p>a white tiger in mid-stride with flowing muscles</p> <p>a Pterodactyl with spread wings in flight pose</p> <p>an orangutan showing intelligent behavior</p> <p>a polar bear with detailed fur texture</p>

Table 3: **Prompt format for 360° object rotation generation.** All prompts follow the same structural template, varying only in the subject description. The subjects are categorized into creative fusion designs that combine different artistic elements and concepts, and natural creatures that focus on realistic animal representations.

A.6. Potential Applications

Our framework demonstrates significant potential beyond its primary applications.

A.6.1. CREATIVE MULTI-VIEW GENERATION

As shown in Figure 10, our method exhibits remarkable flexibility in combining different conceptual elements to create novel multi-view compositions. The grid-based layout allows for intuitive arrangement and manipulation of various visual elements, enabling creative expressions that would be challenging for traditional approaches. This capability suggests promising applications in creative design, artistic visualization, and content creation.

A.6.2. FLEXIBLE FRAME EXTENSION

Notably, our model demonstrates strong generalization capability in sequence length. Despite being trained on 4×4 (16-frame) driving scenarios, the model can effectively generate 4×8 (32-frame) sequences by simply adjusting the *c_{layout}* prompt at inference time. As shown in Figure 11, the extended sequences maintain temporal consistency and visual quality comparable to the original training length. This flexibility suggests that our layout-based approach naturally accommodates variable-length generation without requiring explicit retraining, opening possibilities for dynamic content generation across different temporal scales.

A.6.3. FUTURE EXTENSION TO VIDEO UNDERSTANDING

Our layout-based framework shows potential in transforming traditional video understanding tasks into image-domain problems. Unlike conventional autoregressive approaches (Bai et al., 2024) that process frames sequentially, our method arranges frames in a grid layout, enabling parallel processing and global temporal modeling. This approach could benefit various video understanding tasks: for video-text retrieval, the layout representation allows direct comparison between video content and text embeddings across all frames simultaneously; for video question answering, it enables the model to attend to relevant frames across the entire sequence without sequential constraints; for video tracking and other analysis tasks, it avoids error accumulation common in traditional sequential processing. While we have not conducted specific experiments in these directions, our framework’s ability to convert temporal relationships into spatial ones through layouts offers a promising alternative to conventional video understanding paradigms, potentially enabling more efficient and effective multi-modal video analysis.

A.6.4. MAINTAINED IMAGE GENERATION ABILITY

Our framework preserves the original Flux model’s image generation capabilities while extending its functionality to handle video sequences. As demonstrated in Figure 13, the model maintains high-quality performance on various image generation tasks such as text-to-image synthesis, image editing, and style transfer. This preservation of original capabilities alongside newly acquired video generation abilities creates a versatile model that can seamlessly handle both single-image and multi-frame tasks. The ability to maintain original image generation quality while adding new functionality demonstrates the effectiveness of our training approach and the robustness of the layout-based framework.

A.7. Limitations

Our approach faces two primary limitations. First, the grid-based layout design inherently constrains frame resolution due to limitations of the based Text-to-Image models when processing multiple frames simultaneously. Second, our training strategy, based on lora finetuning, shows limitations in text-to-video generation tasks that significantly deviate from the base model’s capabilities. Combined with our relatively small training dataset, this makes it challenging to achieve competitive performance in open-world video generation scenarios requiring complex motion understanding.

A.8. Multiview Camera Parameters

Building upon the dataset opensourced by Diffusion4D (Liang et al., 2024), Table 4 presents camera trajectory parameters, which serve as the foundation for consistent 4D content generation and subsequent reconstruction tasks.

Our camera configuration follows precise mathematical relationships, with cameras positioned at 15-degree intervals along a circle of radius 2 units in the horizontal plane. The systematic progression of coordinate bases ensures optimal coverage

Frame	X Vector	Y Vector	Z Vector	Origin
1	[1.0, 0.0, 0.0]	[-0.0, 0.0, -1.0]	[-0.0, 1.0, 0.0]	[0.0, -2.0, 0.0]
2	[0.96, 0.27, -0.0]	[0.0, -0.0, -1.0]	[-0.27, 0.96, -0.0]	[0.54, -1.93, 0.0]
3	[-0.92, 0.4, -0.0]	[0.0, 0.0, -1.0]	[-0.4, -0.92, -0.0]	[0.8, 1.83, 0.0]
4	[-0.99, 0.14, -0.0]	[0.0, 0.0, -1.0]	[-0.14, -0.99, -0.0]	[0.27, 1.98, 0.0]
5	[-0.99, -0.14, 0.0]	[-0.0, 0.0, -1.0]	[0.14, -0.99, -0.0]	[-0.27, 1.98, 0.0]
6	[-0.92, -0.4, 0.0]	[-0.0, 0.0, -1.0]	[0.4, -0.92, -0.0]	[-0.8, 1.83, 0.0]
7	[-0.78, -0.63, 0.0]	[-0.0, -0.0, -1.0]	[0.63, -0.78, 0.0]	[-1.26, 1.55, 0.0]
8	[-0.58, -0.82, -0.0]	[0.0, 0.0, -1.0]	[0.82, -0.58, 0.0]	[-1.63, 1.15, 0.0]
9	[-0.33, -0.94, -0.0]	[0.0, -0.0, -1.0]	[0.94, -0.33, 0.0]	[-1.88, 0.67, 0.0]
10	[-0.07, -1.0, -0.0]	[0.0, 0.0, -1.0]	[1.0, -0.07, 0.0]	[-2.0, 0.14, 0.0]
11	[0.2, -0.98, 0.0]	[0.0, -0.0, -1.0]	[0.98, 0.2, 0.0]	[-1.96, -0.41, 0.0]
12	[0.46, -0.89, 0.0]	[0.0, -0.0, -1.0]	[0.89, 0.46, 0.0]	[-1.78, -0.92, 0.0]
13	[0.85, 0.52, 0.0]	[-0.0, 0.0, -1.0]	[-0.52, 0.85, 0.0]	[1.04, -1.71, 0.0]
14	[0.68, -0.73, -0.0]	[-0.0, 0.0, -1.0]	[0.73, 0.68, 0.0]	[-1.46, -1.37, 0.0]
15	[0.85, -0.52, -0.0]	[0.0, 0.0, -1.0]	[0.52, 0.85, 0.0]	[-1.04, -1.71, 0.0]
16	[0.96, -0.27, 0.0]	[-0.0, -0.0, -1.0]	[0.27, 0.96, -0.0]	[-0.54, -1.93, 0.0]
17	[1.0, -0.0, 0.0]	[0.0, 0.0, -1.0]	[0.0, 1.0, 0.0]	[-0.0, -2.0, 0.0]
18	[0.68, 0.73, 0.0]	[0.0, 0.0, -1.0]	[-0.73, 0.68, 0.0]	[1.46, -1.37, 0.0]
19	[0.46, 0.89, -0.0]	[-0.0, -0.0, -1.0]	[-0.89, 0.46, 0.0]	[1.78, -0.92, 0.0]
20	[0.2, 0.98, -0.0]	[-0.0, -0.0, -1.0]	[-0.98, 0.2, 0.0]	[1.96, -0.41, 0.0]
21	[-0.07, 1.0, 0.0]	[-0.0, 0.0, -1.0]	[-1.0, -0.07, 0.0]	[2.0, 0.14, 0.0]
22	[-0.33, 0.94, 0.0]	[-0.0, -0.0, -1.0]	[-0.94, -0.33, 0.0]	[1.88, 0.67, 0.0]
23	[-0.58, 0.82, 0.0]	[-0.0, 0.0, -1.0]	[-0.82, -0.58, 0.0]	[1.63, 1.15, 0.0]
24	[-0.78, 0.63, -0.0]	[0.0, -0.0, -1.0]	[-0.63, -0.78, 0.0]	[1.26, 1.55, 0.0]

Table 4: Camera Parameters for 24 Frames

while maintaining consistent inter-frame relationships. Each camera’s orientation is defined by orthogonal basis vectors, with the Y vector consistently aligned with the negative Z-axis to establish stable up-direction reference.

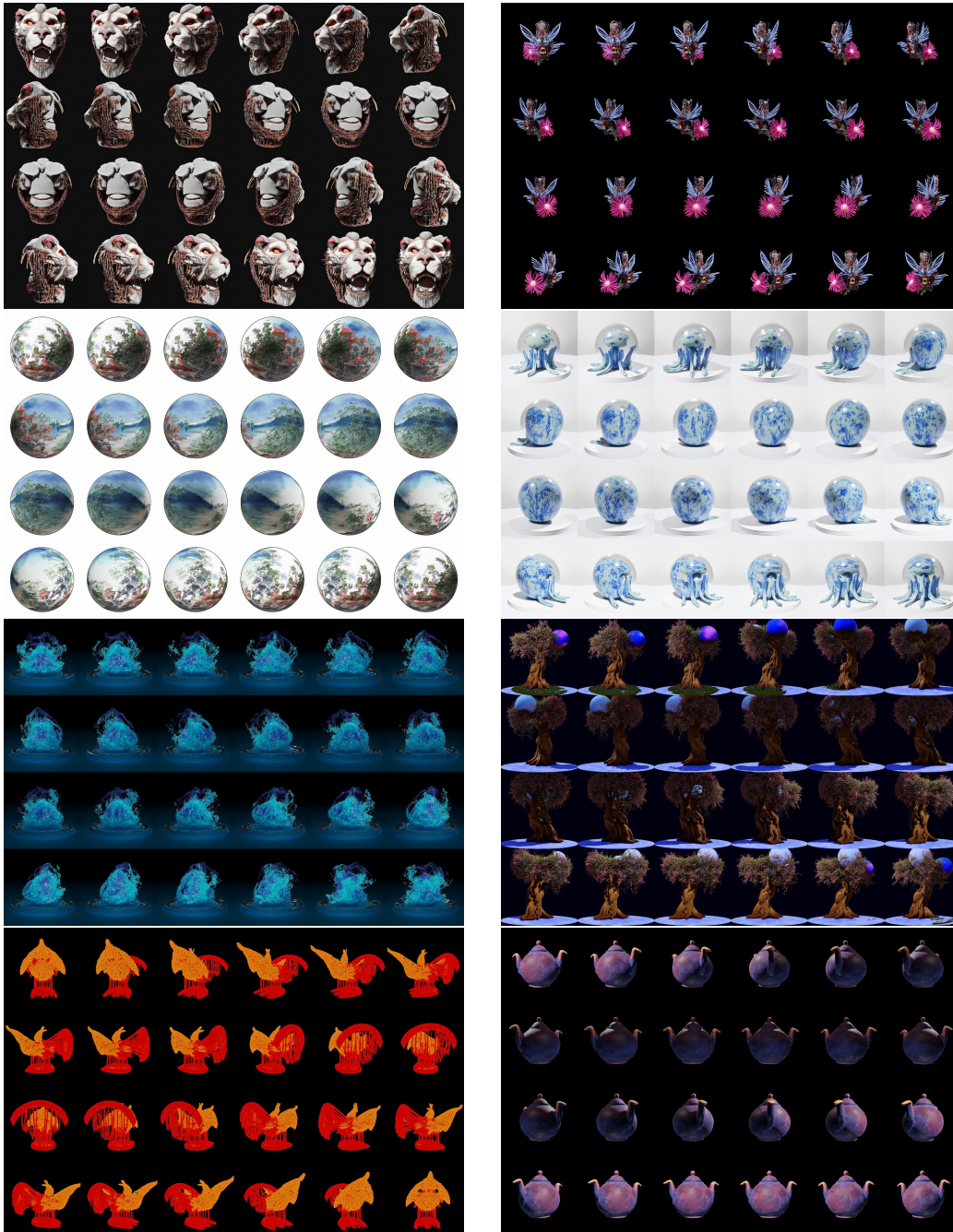


Figure 10: Creative multi-view concept generation.



Figure 11: We only train our model using 4×4 datasets, but when at inference, we directly change prompt to ask to layout 4×8 grid. The model has not trained on these kind of dataset, but show a zero-shot generalization ability.

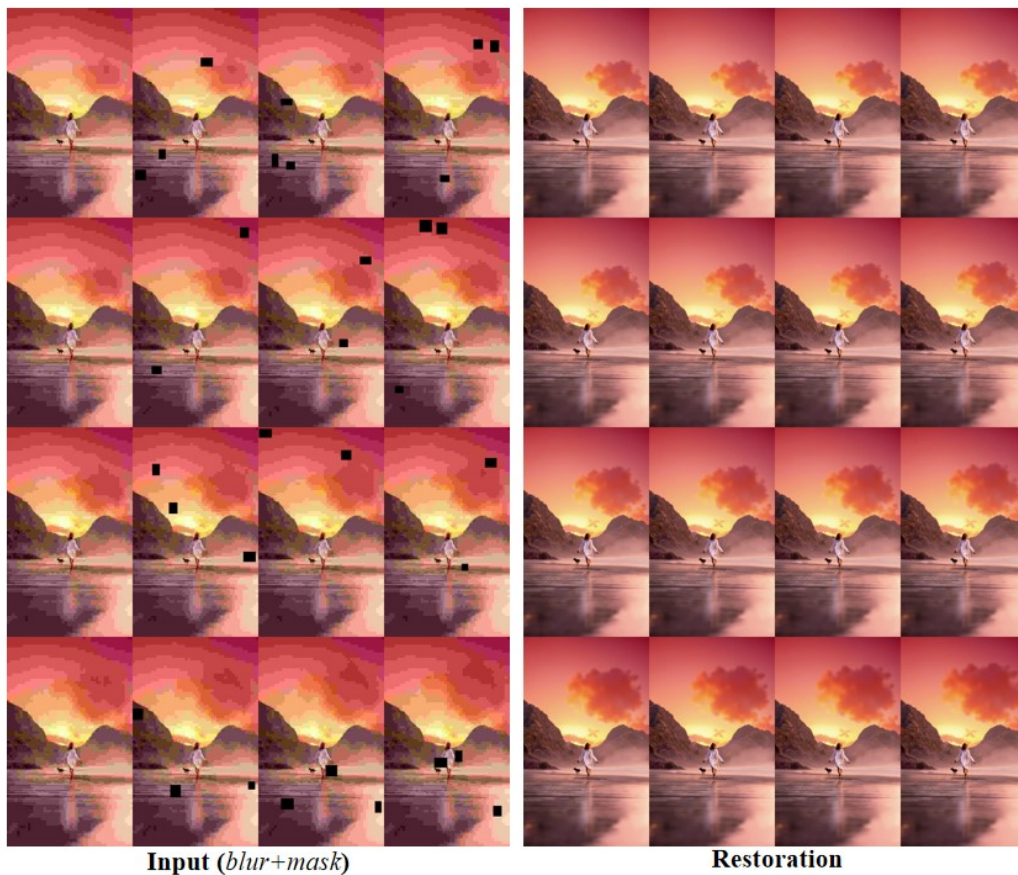


Figure 12: Video restoration from degraded inputs. Left: Input sequences with Gaussian blur and block masking. Right: Restored high-quality outputs maintaining temporal consistency.

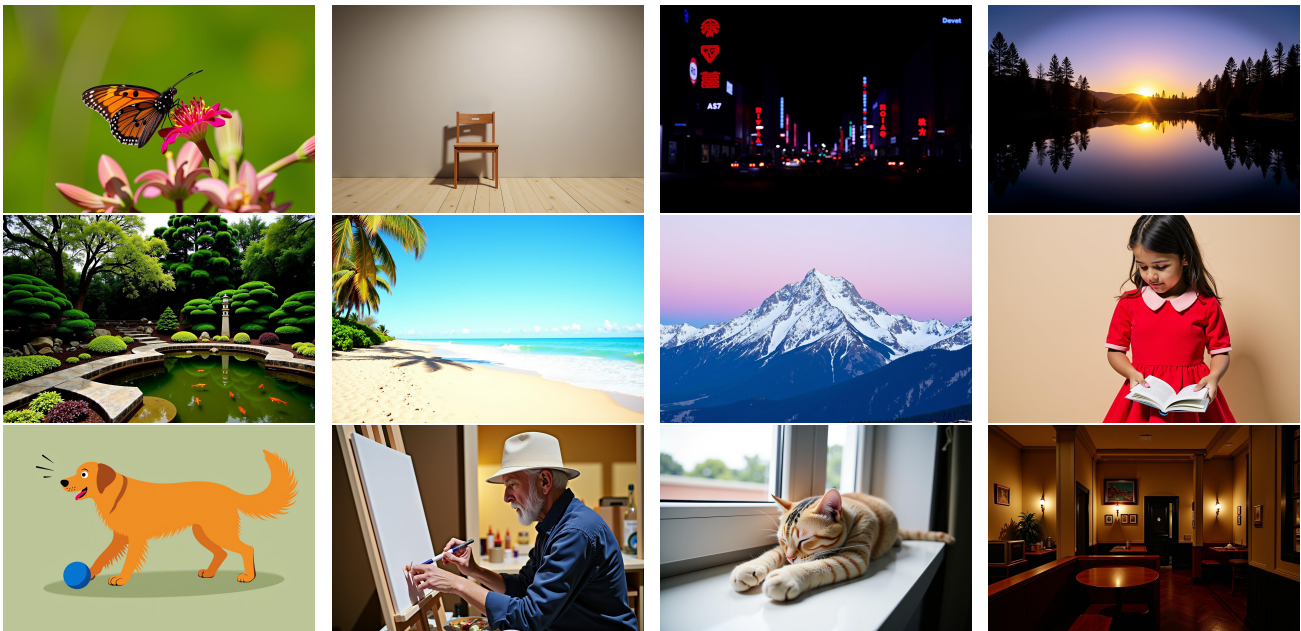


Figure 13: Demonstration of maintained image generation capabilities. Our model preserves high-quality single-image generation performance across diverse scenarios including: basic objects, nature scenes, character interactions, indoor/outdoor environments, artistic styles, and lighting effects. Each image is generated from text prompts testing different aspects of the model’s generation abilities.